

Study the Percentage of Carbon and Ferrite in Layers of Steel (SA-516) by Strip Cladding with E316L

Ahmad Afsari^{1*}, Dara Fazel¹, Jafar Karimisharifabadi¹, Vahid Mehrabi¹

¹Department of Mechanical Engineering, Shiraz Branch, Islamic Azad University, Shiraz, Iran

*Email of Corresponding Author: afsari@iaushiraz.ac.ir

Received: June 14, 2020; Accepted: September 9, 2020

Abstract

One of the most important methods to reduce metal corrosion and improve erosion resistance is to use strip cladding with electro slag welding. Applying the strip electrode (E316L), cladding performed on the layer of steel (SA-516) with this process. With changes in the thickness of cladding layers and the number of these layers, the percentages of ferrite and carbon in samples obtained by WRC equipment were analyzed. The optical microscopy is used to investigate the microstructure of different cladding layers in this research work. Hence, with the increase in the percentage of carbon, the sensitivity of stainless steel to grain boundary corrosion increases. With the reduction of ferrite percentage, the sensitivity to hot cracking increased too, so the overall results indicate that with an increase in the thickness of the first cladding layer, the amount of carbon in this layer increases, this phenomenon reduces the percentage of ferrite in it. Hence, by increasing the number of cladding layers, the amount of carbon percentage reduces considerably while the ferrite percentage reaches the desired amount.

Keywords

Cladding, Electro Slag Welding, Stainless Steel, Carbon Ferrite Percentage, Strip Electrode

1. Introduction

The creation of coating by the welding method is used today in most industries to prevent wear and corrosion. The coating process with electrolytic strip slag welding due to its high speed and controlled input temperature is well known, and because of its economic benefits, it has been widely used in various industries. This process is based on the process of coating with submerged arc welding with strip electrode, which is extensively used in oil, gas, and petrochemical industries to cover the internal surfaces of pressure vessels, reactors, heat exchangers, and other equipment. There are various methods for reducing the corrosion of metals and also increasing the wear resistance of metals. Many researchers have examined the impact of coating on factors such as wear resistance, corrosion resistance, and fracture toughness. Research indicates that increasing the intensity of current and reducing the feed speed of the device will increase the degree of dilution or increase the percentage of alloy elements of base metal in the coating layer of the stainless steel 316L [1]. The temperature process, such as submerged arc powder coatings, striped slag electrical coatings, plasma coatings, and the like, are examples of the objectives mentioned. However,

unfortunately, most of these processes result in the melting of the underlying coatings or lead to problems such as hot cracks, porosity, separation, melting of microstructures, and the formation of unnecessary phases in the coating area [2, 3 & 6]. Also, the process of gas metal arc welding (GMAW) used for coating, the boron enriched on steel ST50 and the results indicate that the composite layer of FeB and F-Fe₂B α formed, which has a strong joint with base metal, while the hardness of the boride particles is higher than 1600 VC. As a result, by increasing the amount of boride, the hardness of the coating layer also increases [4]. In another study in the TIG welding process, a metal-coated electrode 316L for coating the equipment has been used. The results of the ultrasonic test show that the anisotropy of the gas tungsten arc welding electrode (GTAW) is more than that of arc welding with a coated metal electrode (SMAW) and, besides, the damping in the arc welding with tungsten electrode with protective gas is of a higher amplitude [5]. The effect of tungsten inert gas welding on the degree of dilution of the coating process with stainless steel has been studied so that by decreasing the feed speed, the degree of dilution increases and the quality of the stainless steel coating layer is reduced [7]. A study was conducted on the properties of austenitic stainless steel whose surface was coated by friction welding [8]. The corrosion behavior of the coat of AISI316L on stainless steel has been investigated, and the results indicate that this type of coating is more resistant to corrosion cracking [9]. In another study, a steel plate of carbon steel A516-G70, clad by the shielded metal arc welding method and the samples with two and three layers, cladding examined. So the results obtained indicate that the maximum amount of residual stresses in the clad layer, are tensile, and in the stress limit, it is in the submission of base metal and cladding layer [10]. The tensile residual stress in cladding is mainly due to the differences in the thermal expansion of the cladding and the base materials. Also, post-weld heat treatment is used to adjust the residual stresses [11].

According to research carried out, it can say with certainty that the coating layers created by electro slag strip welding are far from the limitations and besides have advantages such as simplicity, ability to be deposited in a wide range of materials, and are also suitable for coating and repairing the surfaces. With the advancement of welding processes, the scope of application of metal coating processes is rapidly developing, and the choice of the type of coating process will be dependent on a variety of factors, such as the coating speed, the heat input to the workpiece, as well as the cost of coating.

2. Materials and Methods

The bandwidth of the strip electrodes used in this study was 16, 30, 60, 90, and 120 mm, and their thickness was 0.5 mm. The powder temperature can reach above 2500°C with bypassing the electrical current from the electrode and then using the protective powder. Consequently, by inserting the electrode into the slag, the electrode melts and creates a uniform coating on the surface of the workpiece. The width of the coating layer is equal to the width of the electrode. However, the thickness of the layer depends on the feed speed of the device and the feeding speed of the strip electrode. The schematic of the electro slag coating device with the strip electrode is shown in Figure 1.

In this study, parameters such as thickness and the number of coating layers on different specimens have been investigated. The above parameters are used to control the percentage of carbon and

ferrite of coated layers. By controlling the percentage of carbon in the coating layers, the sensitivity of the corrosion resistance of the grain boundary layer is controllable and, by controlling the ferrite percentage within the appropriate range, the sensitivity of hot crack controlled according to the Welding Research Council (WRC) graph, Figure 2 shows the WRC graph.

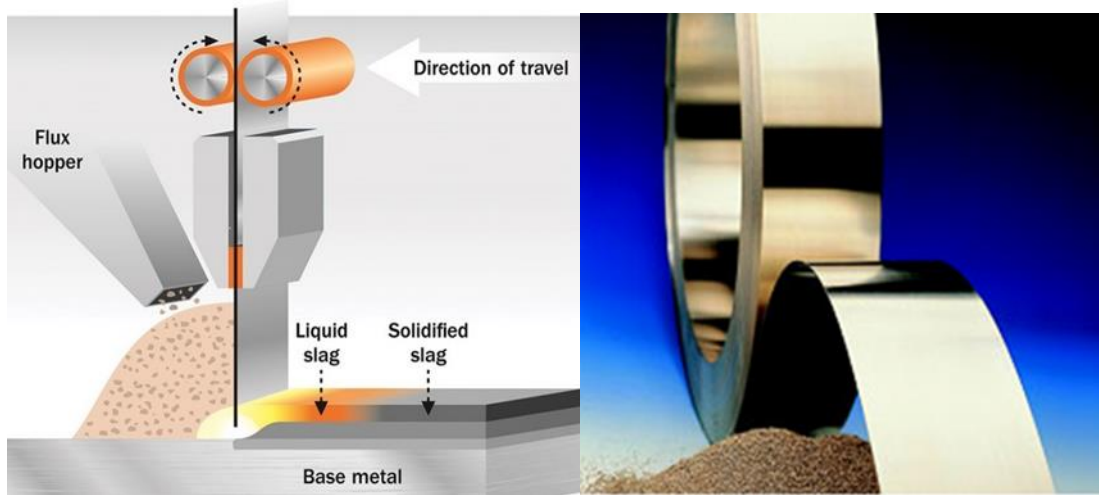


Figure 1. An electro slag coating machine with a strip electrode and coated pressure vessel surface

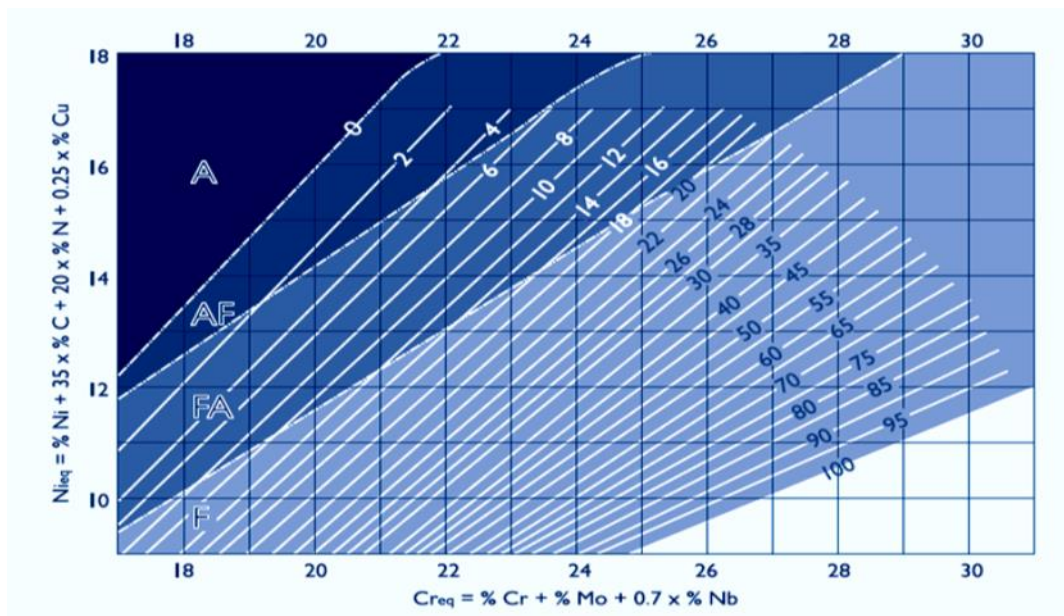


Figure 2. The Schematic diagram of the WRC

The coating operation was performed by the electro slag stripper ESAB. To prepare the specimens for coating operation, initially, a sheet of carbon steel SA-516 with the dimensions of 800 × 150 mm and a thickness of 20 mm was selected and then cut by a plasma cutting machine to 4 samples with the dimensions of 200 × 150 × 200 mm, and then the surfaces of the specimens were ground to eliminate the oxide layers. The chemical composition of the sheet specimen is given in Table 1.

Table 1. Chemical composition of carbon steel SA-516, ASME Sec: II Part-A standard

Chemical composition of the sheet SA516 Gr-70								
S	Nb	MN	Pb	Cu	Ni	C (Max.)	C (Min.)	Fe
0.035	0.067	1.3	0.07	0.07	0.07	0.28	0.18	Bal.

Based on variables parameters, including the feed speed of the device, the feeding speed of the strip electrode, the intensity of the current, the voltage, the thickness of the layers, the type of electrode, and the number of coated layers, Samples prepared, and specification of coated specimen and variables parameters of the experimental work recorded in Table 2 for each of the coating layers. In this regard, Parameters such as ampere, voltage, and feeder speed of the strip electrode to be considered constant. In this regard, the electrode 309L was used for the first layer of coating in all four samples because this type of electrode is usually used for the welding of dissimilar specimens of steel materials.

Table 2. Specification of Specimen coated layer

Samples	Sample No.: 1		Sample No.: 2		Sample No.: 3		Sample No.: 4		
	Coated layer		Coated layer		Coated layer		Coated layer		
	No.:		No.:		No.:		No.:		
Type of Electrode	309L	316L	309L	316L	309L	316L	309L	316L	316L
Layer thickness (mm)	5	2	3.5	3.5	2	5	2	2.5	2.5
Voltage (V)	28	28	28	28	28	28	28	28	28
Current Intensity (A)	800	800	800	800	800	800	800	800	800
Electrode feed (cm/Min.)	400	400	400	400	400	400	400	400	400
Machine feed (cm/Min.)	16	35	26	26	35	16	35	19	19

After the operation, the thickness of each of the coated layers measured at each step by the thickness measurement gauges, shown in Figure 3. The total thickness of the coating layers in each of the four samples is 7 mm. The only sample that is coated with three layers is the fourth one.

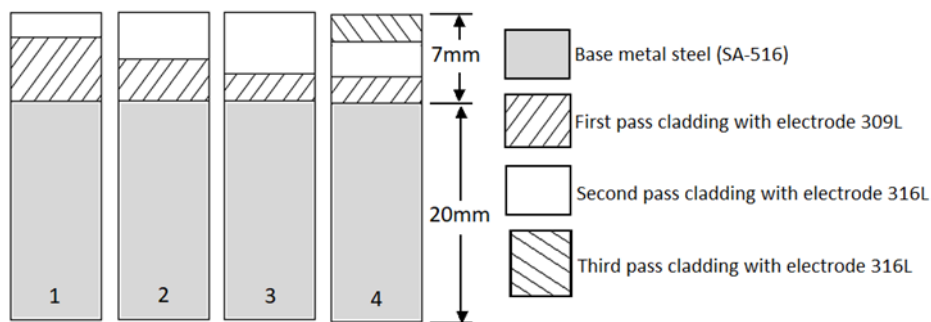


Figure 3. The thickness of the coated layers of different samples

After completing the cladding operation and before the performance of destructive tests, all samples inspected by the liquid penetrant inspection process for tracking the surface cracks. An ultrasonic inspection process is used to verify the discontinuities between the coated layer and the base metal.

The results show that no superficial cracking or discontinuity between the coated layers and the base metal. Figure 4 shows the ultrasonic device used for this purpose.



Figure 4: Ultrasonic device for tracking discontinuity

After ensuring the correct formation of the coated layers, the samples are cut by Electro Discharge Wire Machine to the dimension of 20 x 20 x 20 mm and then, to determine the percentage of alloying elements from the surface of the coated layer, the quantum device was used, which shown in Figure 5, the specifications presented in Table 3. For more certainty and to prevent possible errors, from each coated sheet, two samples were selected and placed in a quantum device to be tested.

Table 3. Specifications of quantum device

Model: Master - Foundry	Number of recognizable elements = 52	Accuracy of the device = 0.0001%
-------------------------	--------------------------------------	----------------------------------



Figure 5. A quantum device to detect alloy elements

For the study, the crystalline structure, the samples were cut transversely by Electro Discharge Wire Machine. Then all the samples were polished and analyzed using an optical microscope with a magnification of 100. Figure 6 shows the crystalline structure of the final or superficial coated layer of four samples. As shown in Example 1 of Figure 6, the final coated layer is dendritic shaped due to the low input heat, the high feed rate of the progression, and the high cooling rate, which is above the austenitic layer. While in samples 2 and 3, due to the higher incoming heat and lower feed rate and the low cooling rate of the layer with austenite structure, the final coated layer has a uniform

and spherical shape. In sample No. 4, due to the low input heat and high feed rate and also the cooling velocity above the austenitic layer, the final coated layer is of fully extendable type and appears as a needle-shaped structure.

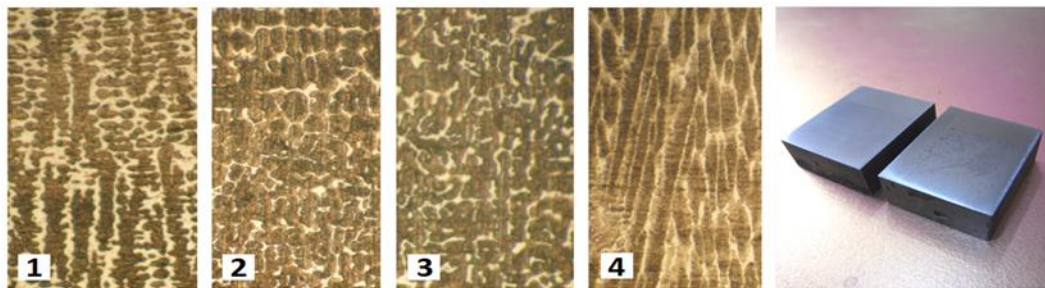


Figure 6. Crystal structure of coated layers of different samples

According to changes in the thickness of the coating layers and the number of coated layers, the Vickers hardness test machine is used to determine the hardness of the coated layers. In this regard, the hardness of the different points of the coating layers, the heat affected area, and the base metal of each of the four samples examined, and the data obtained in the form of a graph shown in Figure 7. The horizontal axis represents the point of the pyramid of the hardness device on the sample. The zero points of the horizontal axis show the surface hardness of the specimen, and the range between zero and seven shows the coverage area of the thickness of the coated layer. Also, point seven represents the interface between the coated layers and the base metal.

3. Results and Discussion

In the experiments performed on the samples, it found that in the process of strip electrode (E316L) cladding with the electro slag method, the thickness of the coated layers increases by reducing the feed speed of the device. Hence, by increasing the thickness of the coating layers, the penetration of the weld will also increase. So, with increasing the depth of the coated layers, the percentage of alloying elements of the layers is also significantly affected, and due to this phenomenon, the quality of the coated layers will also be affected.

By examining the carbon percentage in the thickness of the first layer of the coating layer, it observed that with increasing the thickness of the first coating layer, the penetration of the weld also increased and lead to increasing the degree of dilution or the increase of the percentage of alloying elements of the base metal into the coating layer. In this regard, the thickness of the first coated layer on the percentage of carbon shown in Figure 7.

As stated, the thickness of the first layer of coating on the ferrite percentage reflects the fact that by increasing the thickness and depth of the first coated layer, the higher percentage of carbon of the base metal, which is of carbon steel type, is brought to the weld metal and causes the significant increases of equivalent nickel into the WRC chart. Besides, by increasing the equivalent nickel, the ferrite percentage in the austenitic metal is reduced, and the coated layer becomes closer to the pure austenite. Therefore, by reduction of the percentage of ferrite and by crossing the border 4%, the sensitivity to hot crack increases. In this regard, the thickness of the first coated layer on the ferrite percentage shown in Figure 8.

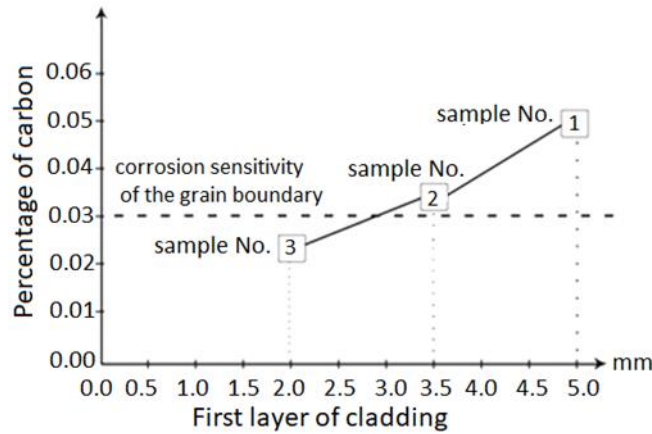


Figure 7. Effect of the thickness of the first cladding layer on the percentage of carbon

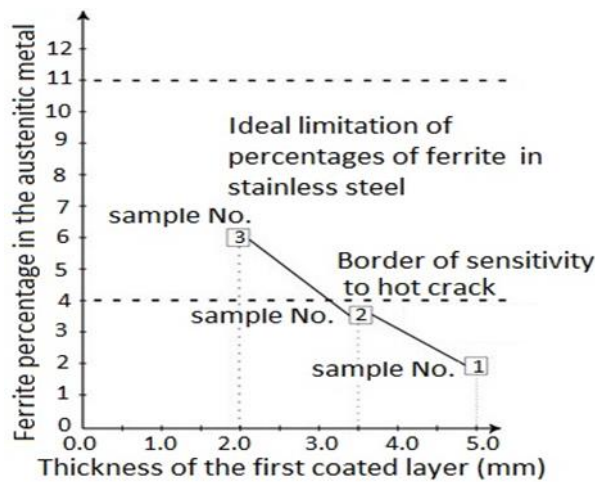


Figure 8. The effect of the thickness of the first cladding layer on the percentage of ferrite

By examining the number of coated layers on the percentage of carbon and ferrite percentage, it can claim that with the constant consideration of the thickness of the first coated layer and the total coated layers, the base metal alloy elements will transfer less to the final surfaces with increasing the number of coating layers. Therefore, it will have a direct impact on the percentage of carbon and ferrite percentage on the final layer of coating. In this regard, increasing the number of coating layers from two layers to three layers of coating on carbon percentage and ferrite percentage is shown in Figures 9 and 10, respectively.

As shown in Fig. 11, the hardness of each of the four specimens in the area affected by the heat and the common area greatly reduced due to the crystalline structure of the base metal. In sample number 1, the sample surface shows a higher hardness because of the high feed speed of the device and the low input temperature of the final coating layer. However, in the underlying layer, due to the high input heat, the low velocity of coating, and the low cooling rate, the hardness of this layer has been severely reduced, with the least hardness.

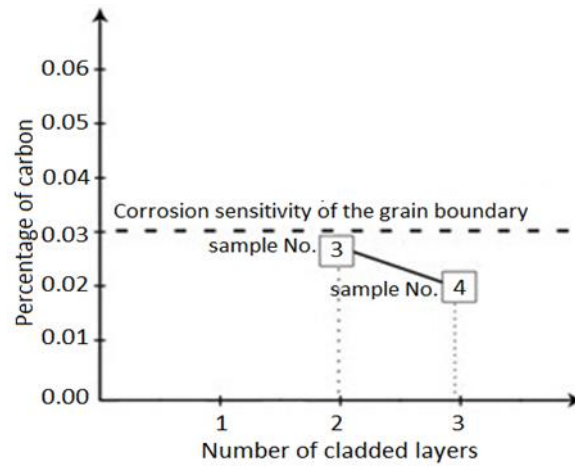


Figure 9. Effect of three cladding layers on the percentage of carbon content

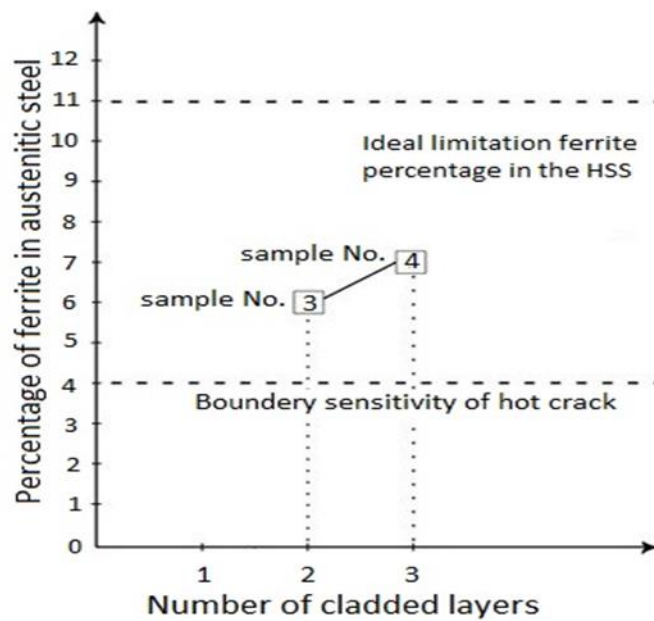


Figure 10. Effect of three coating layers on the percentage of ferrite.

In sample No. 2, the hardness of both coated layers is in the range of 160 to 180 Vickers. In sample No. 3, due to the very high thermal input of the final coating layer, the surface hardness of the sample and the hardness of the underlying layer significantly decreased. In sample No. 4, due to the low input heat in all three coated layers, it has a higher hardness than the other specimens, and the relative hardening of the lower layers in this sample is due to the reheating of the higher layers.

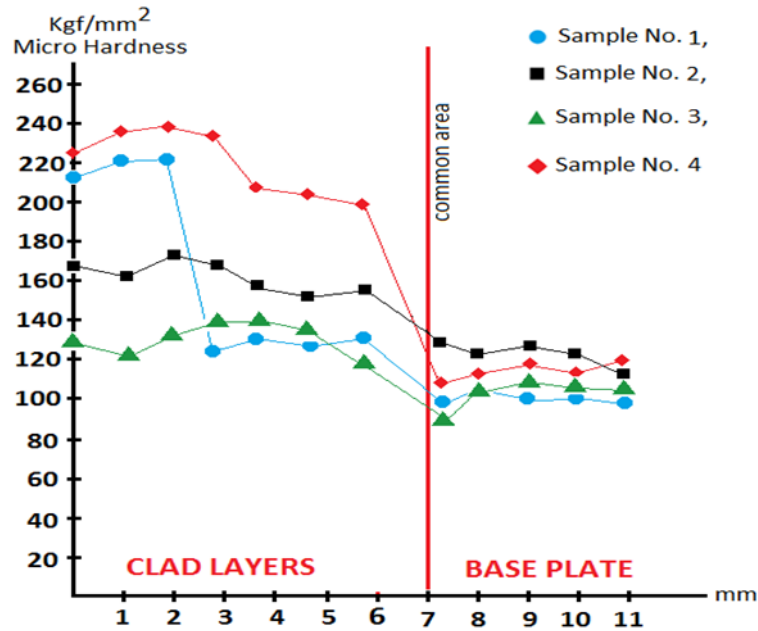


Figure 11. Hardness diagram of cladding layers

4. Conclusion

- By examining the change in the percentage of carbon in the thickness of the first layer and also the increase in the number of coating layers, the results show that by increasing the thickness of the first layer of coating, the percentage of carbon increases, and in this connection, with increasing the number of coatings layers, carbon percentage decreases in the last layer of coating, as a result, the corrosion sensitivity of the grain boundary reduced.
- With the change in the thickness of the first coating layer and the increase in the number of coating layers, the percentage of ferrite investigated, and the results show that with increasing thickness of the first coating layer, the ferrite percentage decreases due to the increase of nickel equivalent. Also, by increasing the number of coating layers, the ferrite percentage increases due to the reduction of nickel equivalent, and as a result, the sensitivity to hot crack will decrease.
- It can claim that by this method that the quality of the coating layers' devices such as high-pressure vessels and reactors can increase by increasing the coating layers, although it increases the cost of coating. Also, decreasing the thickness in the first layer of coating, the quality of the coating layers was improved, leading to an increase in the useful life of the equipment against corrosive and warm fluids.
- By reducing the inlet heat or increasing the coating speed, the spherical and uniform structure shape converted into a stretched and needle structure. Also, by increasing the number of coating layers in a way that does not change the overall thickness of the coating layers, the structure will turn from spherical to quadratic or needle structure.
- By reducing the input heat and high coating feed speed, in other words, reducing the thickness of the coating layers, the cooling rate increases and increases the hardness of the coating layers.

- In the case of stomatal corrosion, this type of coating has more resistance than other coating methods.

5. References

- [1] Chiu, K.Y., Cheng, F.T. and Man, H.C. 2006. Corrosion behavior of AISI 316L stainless steel surface-modified with NiTi. *Surface and Coatings Technology*. 200(20-21):6054-61.
- [2] Vitanov, V.I., Javaid, N. and Stephenson, D.J. 2010. Application of response surface methodology for the optimization of micro friction surfacing process. *Surface and Coatings Technology*. 204(21-22):3501-3508.
- [3] Khalid Rafi, H., Janaki Ram, G.D., Phanikumar and G., Rao, K.P. 2010. Microstructure and properties of friction surfaced stainless steel and tool steel coatings. *Materials Science Forum*. 638: 864-869.
- [4] Amushahi, M.H., Ashrafizadeh, F. and Shamanian, M. 2010. Characterization of boride-rich hard facing on carbon steel by arc spray and GMAW processes. *Surface and Coatings Technology*. 204(16-17):2723-2728.
- [5] Tabatabaeipour, S.M. and Honarvar, F. 2010. A comparative evaluation of ultrasonic testing of AISI 316L welds made by shielded metal arc welding and gas tungsten arc welding processes. *Journal of materials processing technology*. 210(8):1043-1050.
- [6] Rafi, H.K., Ram, G.J., Phanikumar, G. and Rao, K.P. 2011. Microstructural evolution during friction surfacing of tool steel H13. *Materials & Design*. 32(1):82-87.
- [7] Rajani, H.Z., Torkamani, H., Sharbati and M., Raygan, S. 2012. Corrosion resistance improvement in Gas Tungsten Arc Welded 316L stainless steel joints through controlled preheat treatment. *Materials & Design*. 34:51-57.
- [8] Govardhan, D., Kumar, A.C., Murti, K.G and Reddy, G.M. 2012. Characterization of austenitic stainless steel friction surfaced deposit over low carbon steel. *Materials & Design*. 36:206-214.
- [9] Puli, R. and Ram, G.J. 2012. Corrosion performance of AISI 316L friction surfaced coatings. *Corrosion Science*. 62:95-103.
- [10] Dehaghi, E.M., Arezoodar, A.F. and Sattarifar, I. 2018. Numerical and Experimental Investigation of Layer Number Effect on Residual Stresses in Cladding Process. 49(4):295-298.
- [11] Katsuyama, J., Nishikawa, H., Udagawa, M., Nakamura, M. and Onizawa, K. 2013. Assessment of residual stress due to overlay-welded cladding and structural integrity of a reactor pressure vessel. *Journal of Pressure Vessel Technology*. 135(5):051402.